FEBS Letters 584 (2010) 2291–2297

FEBS Letters

journal homepage: www.FEBSLetters.org

ROS leads to MnSOD upregulation through ERK2 translocation and p53 activation in selenite-induced apoptosis of NB4 cells

Zhushi Li, Kejian Shi, Liying Guan, Tingming Cao, Qian Jiang, Yang Yang, Caimin Xu *

National Laboratory of Medical Molecular Biology, Institute of Basic Medical Sciences, Peking Union Medical College and Chinese Academy of Medical Sciences, Beijing 100005, China

ARTICLE INFO

Article history:
Received 1 January 2010
Revised 25 March 2010
Accepted 26 March 2010
Available online 28 March 2010

Edited by Vladimir Skulachev

Keywords:
Manganese superoxide dismutase
Reactive oxygen species
Extracellular regulated kinase
Nuclear translocation
p53

ABSTRACT

Following our previous finding that sodium selenite induces apoptosis in human leukemia NB4 cells, we now show that the expression of the critical antioxidant enzyme manganese superoxide dismutase (MnSOD) is remarkably elevated during this process. We further reveal that reactive oxygen species (ROS), especially superoxide radicals, play a crucial role in selenite-induced MnSOD upregulation, with extracellular regulated kinase (ERK) and p53 closely implicated. Specifically, ERK2 translocates into the nucleus driven by ROS, where it directly phosphorylates p53, leading to dissociation of p53 from its inhibitory protein mouse double minute 2 (MDM2). Active p53 directly mediates the expression of MnSOD, serving as the link between ERK2 translocation and MnSOD upregulation.

1. Introduction

Selenium is one of the essential trace elements with anti-tumor properties. Supranutritional selenium compounds are able to trigger apoptosis in diverse tumor cell lines [1–3]. In our previous work, we found 20 μmol/l of sodium selenite-induced pronounced apoptosis in NB4 cells derived from human acute promyelocytic leukemia (APL), while reactive oxygen species (ROS) played a critical role [4–9]. Here we discovered dramatically elevated expression of manganese superoxide dismutase (MnSOD) during this process. Mainly located in mitochondrial matrix, MnSOD is well known as one of the major antioxidant enzymes against superoxide free radicals, and catalyzes dismutation of superoxide radical anion into hydrogen peroxide, protecting cells from damage of oxidative stress [10,11]. Therefore MnSOD upregulation seems an important protective mechanism by which NB4 cells counteracts ROS-mediated injuries.

As to the detailed mechanisms of MnSOD upregulation, we elucidated that extracellular regulated kinase (ERK) and p53 were closely involved. ERK participates in a variety of cellular activities including proliferation, differentiation, cycle progression, aging, migration, cytoskeleton formation as well as apoptosis by phosphorylating extensive target proteins. ERK2 and ERK1 are predominant members of this family with highly similar structures and functions [12,13]. ERK is capable of entering the nucleus to exert the functions of cell death repression and cell cycle entry [14–17]. As another important factor, p53 is known as one of the most crucial tumor suppressors with the ability to block cell cycle, initiate DNA repair, accelerate cell aging and induce apoptosis [18]. Also, as a transcription factor, p53 regulates a series of target genes including sod2 which encodes MnSOD [19,20]. According to the previous research [21–24], as well as the data from our cDNA sequencing analysis, NB4 cells express a wild-type p53. Here we demonstrated that ERK2 was translocated into the nucleus driven by ROS, where it directly bound to and phosphorylated p53 at the vital site Ser15. Consequently, p53 dissociated from its inhibitory protein mouse double minute 2 (MDM2) and contributed to augmented expression of MnSOD. Additionally, in leukemia cell lines with null or mutant p53 such as HL-60 and U937, selenite could not induce the upregulation of MnSOD, further corroborating the critical role of p53 in this modulation.

2. Materials and methods

2.1. Cell culture

NB4, HL-60 and U937 cells were cultured in RPMI 1640 culture medium (Gibco, USA) supplemented with 10% fetal bovine serum,

Abbreviations: APL, acute promyelocytic leukemia; MnSOD, manganese superoxide dismutase; ROS, reactive oxygen species; ERK, extracellular regulated kinase; MDM2, mouse double minute 2

* Corresponding author. Fax: +86 10 65296445.
E-mail address: caiminxu@yahoo.com.cn (C. Xu).

0014-5793/$36.00 © 2010 Federation of European Biochemical Societies. Published by Elsevier B.V. All rights reserved.
doi:10.1016/j.febslet.2010.03.040

0.2% sodium bicarbonate, 100 units/ml penicillin and 100 μg/ml streptomycin in a humidified 5% CO_2 atmosphere at 37 °C.

2.2. Reagents and antibodies

Sodium selenite (purity 98%) was purchased from Sigma–Aldrich (St. Louis, MO, USA). Antibody to MnSOD was purchased from BD Transduction Laboratories (Lexington, KY, USA). Antibodies to ERK2, B23, MDM2 and Bax were purchased from Santa Cruz Biotechnology (Santa Cruz, CA, USA). Antibodies to phospho-ERK1/2 (Thr202/Tyr204), p53 and phospho-p53 (Ser15) were purchased from Cell Signaling Technology (Danvers, MA, USA). Antibody to β-actin was purchased from Sigma–Aldrich. The chemical inhibitors SB203580, SP600125 and PD98059 were purchased from Promega (Madison, WI, USA). MnTMPyP and Pifithrin-α were purchased from Calbiochem (San Diego, CA, USA).

2.3. Cell lysis and Western blot analysis

About 1×10^7 cells were collected and washed twice with ice-cold PBS. The harvested cells were lysed in cell lysis buffer RIPA (20 mM Tris pH 7.5, 150 mM NaCl, 1 mM EDTA, 1 mM EGTA, 1% Triton X-100, 2.5 mM sodium pyrophosphate, 1 mM β-glycerol-phosphate, 1 mM Na_3VO_4, 1 μg/ml leupeptin, 1 mM PMSF) and subjected to sonication for 30 s. The cell lysates were centrifuged at 12 000×*g* for 25 min at 4 °C and the supernatant was collected. Bradford Assay was used to determine the protein concentration. After normalized, equal amounts of proteins were subjected to 15% SDS–PAGE and transferred to nitrocellulose membranes. The membranes were blocked with 5% non-fat milk in TBST and incubated with primary antibodies at 4 °C overnight. After washed with TBST, membranes were incubated with HRP-conjugated secondary antibodies for 90 min at room temperature. After a second washing with TBST, the blots were probed with SuperSignal Chemiluminescent substrate (Thermo Scientific, USA) to visualize the immunoreactive bands.

2.4. p53 cDNA sequencing

Total RNA of NB4 cells was extracted using Trizol reagents (Invitrogen, CA, USA). Then RNA was reverse-transcribed into cDNA using M-MLV reverse transcriptase (Promega). Three pairs of primers were used to cover the whole protein coding region of p53 cDNA. Fragment 1: 5′-GGG GAC ACT TTG CGT TCG-3′ and 5′-TGA CTG CTT GTA GAT GGC-3′, 591 bp product, covering entire exon 2–4 and parts of exon 1 and 5. Fragment 2: 5′-TTC CGT CTG GGC TTC TTG-3′ and 5′-TGG GCA TCC TTG AGT TCC-3′, 737 bp product, covering entire exon 5–9 and parts of exon 4 and 10. Fragment 3: 5′-CGG CGC ACA GAG GAA GAG AAT C-3′ and 5′-CGC ACA CCT ATT GCA AGC AAG GG-3′, 445 bp product, covering entire exon 9–10 and parts of exon 8 and 11. cDNA samples were subjected to PCR amplification using La Taq Polymerase (Takara Biotechnology, Dalian, China) with the following conditions: denaturation at 94 °C for 10 min, 30 cycles each including denaturation at 94 °C for 30 s, annealing at 55 °C for 30 s and extension at 72 °C for 1 min, followed by a final extension at 72 °C for 10 min. The PCR products were sequenced by Invitrogen (Shanghai, China).

2.5. Extraction of cytoplasmic and nuclear fractions

About 1×10^7 cells were collected and washed twice with ice-cold PBS. The harvested cells were lysed in nuclear protein extraction buffer A (Boster Biological Technology, Wuhan, China) on ice for 30 min. Then the cell lysates were centrifuged at 12 000×*g* for 10 min at 4 °C and the supernatant was collected as the cytoplasmic fractions. The pellet was lysed in nuclear protein extraction buffer B (Boster Biological Technology) on ice for 30 min. Then the lysates were centrifuged at 12 000×*g* for 10 min at 4 °C and the supernatant was collected as the nuclear fractions. PMSF and leupeptin were added into buffer A and buffer B before use.

2.6. Immunofluorescent staining

About 1×10^6 cells were collected and washed twice with ice-cold PBS. The harvested cells were transferred to slides, fixed in freshly prepared 4% formaldehyde for 10 min, subjected to permeabilization with 1% Triton X-100 for 30 min. Then the cells were incubated with primary antibody (1:50 dilution) at 4 °C overnight and TRITC conjugated goat anti-rabbit IgG or FITC conjugated goat anti-mouse IgG (1:50 dilution) for 1 h at room temperature. After washed with PBS, cells were stained with DAPI (Sigma–Aldrich) for 5 min. Then the slides were mounted with Fluo-antifading medium (Genmed, Shanghai, China). Image observation and capture were immediately performed using a TE2000-U Nikon Eclipse microscope (Nikon, Tokyo, Japan).

2.7. Immunoprecipitation

Nuclear fractions were extracted as described above. Bradford Assay was used to determine the protein concentration. Sufficient amount of p53 antibody was added into 200 μg proteins and gently rotated at 4 °C overnight. The immunocomplex was captured by adding 25 μl protein A+G agarose beads (Beyotime, Jiangsu, China) and gently rotating at 4 °C for 3 h. Then the mixture was centrifuged at 1500×*g* for 5 min at 4 °C and the supernatant was discarded. The precipitate was washed for three times with ice-cold RIPA buffer, resuspended in 3× sample buffer and boiled for 5 min to dissociate the immunocomplex from the beads. The supernatant was collected by centrifugation and subjected to Western blot (8% SDS–PAGE).

2.8. siRNA transfection

The small interference RNA (siRNA) targeting p53 (5′-CUACU UCCUG AAAAC AACGTT-3′) [25] and non-silencing scrambled siRNA were synthesized by GenePharma (Shanghai, China). About 3×10^6 cells were collected and washed with serum-free grow medium without antibiotics. Then the cells were transfected with 100 or 200 nmol/l siRNA using Opti-MEM reduced serum medium (Gibco) and DMRIE-C reagent (Invitrogen). A subsequent transfection after 24 h was performed to promote p53 inhibition. Then cells were treated with 20 μmol/l sodium selenite for 24 h.

2.9. Flow cytometric analysis of cell apoptosis using Annexin V-FITC/PI staining

The detection was performed according to the manual of Annexin V-FITC apoptosis detection kit (Calbiochem). About 1×10^6 cells were collected, washed with ice-cold PBS, and resuspended in the binding buffer containing suitable amount of Annexin V-FITC. Cells were incubated in the dark for 15 min at room temperature, then the buffer was removed by centrifugation. The cells were resuspended in the binding buffer containing propidium iodide (PI). Then flow cytometric analysis was immediately performed to detect apoptosis.

2.10. ROS measurement

About 3×10^5 cells were harvested, washed with serum-free RPMI culture medium and incubated with 5 μmol/l dichlorofluorescein diacetate (DCFH-DA, Beyotime) or dihydroethidium (DHE, Beyotime) at 37 °C for 30 min. Then the cells were harvested,

washed and resuspended in serum-free RPMI culture medium with or without 20 μmol/l sodium selenite. DCF or DHE fluorescence distribution was recorded each hour by a fluorospectrophotometer for up to 20 h (DCF: excitation wavelength 488 nm and emission wavelength 535 nm, DHE: excitation wavelength 325 nm and emission wavelength 610 nm).

2.11. Statistical analysis

Data were analyzed by two-tailed student's *t*-test. A value of $P < 0.05$ was considered statistically significant.

3. Results

3.1. MnSOD was upregulated through ROS in selenite-induced apoptosis and ERK was involved in this upregulation

Apparent apoptosis of NB4 cells induced by 20 μmol/l of sodium selenite was indicated by Annexin V-FITC/PI staining (Fig. 1A). During this process, two intracellular ROS, superoxide and hydrogen peroxide were detected by dihydroethidium (DHE) and dichlorohydrofluorescein (DCF) assay respectively. The results demonstrated that both of them were notably increased shortly after selenite exposure, but the superoxide radicals declined obviously after 12 h, whereas the hydrogen peroxide maintained a relatively high level (Fig. 1B). In addition, expression of MnSOD, was induced in both dose-dependent (Fig. 1C) and time-dependent (Fig. 1D) manners, suggesting a protective mechanism initiated by NB4 cells against oxidative stress. Notably, after the depletion of ROS by the cell-permeable ROS scavenger MnTMPyP, elevated expression of MnSOD dismissed completely (Fig. 1E and F), indicating a key role of ROS in MnSOD upregulation. Specifically, to substantiate whether the various critical kinases were implicated in MnSOD upregulation, different selective kinase inhibitors were used. Prior to selenite exposure, cells were pretreated with SB203580, SP600125 and PD98059, which specifically inhibited p38MAPK, JNK and ERK respectively. The results showed that SB203580 and SP600125 had no obvious effects on selenite-induced MnSOD expression (Supplementary Fig. 1A), while PD98059 entirely reversed it (Supplementary Fig. 1B and C), indicating a significant regulatory role of ERK.

3.2. Selenite-induced nuclear translocation of ERK2 through ROS

To define the detailed role of ERK in MnSOD upregulation, we extracted cytoplasmic and nuclear fractions of NB4 cells, and detected distribution of ERK2 between these two compartments. A remarkable translocation of total ERK2 and the active form phosphorylated ERK1/2 into the nucleus from the cytoplasm was observed since an early stage (Fig. 2A). Such translocation was entirely abrogated by ROS scavenger MnTMPyP (Fig. 2B and C), indicating the driving force of ROS. This was further confirmed by immunofluorescent staining, through the co-localization of ERK2 and DAPI in the merged image after selenite exposure, which was completely cancelled by MnTMPyP (Fig. 2D). Considering the critical function of ERK for MnSOD upregulation and the importance of nucleus for regulating protein expression, we hypothesized that the nuclear translocation of ERK2 was probably a critical process closely related with MnSOD upregulation.

3.3. ERK2 phosphorylated and activated nuclear p53 after its translocation

We inferred from the results described above that there must be some links between ERK2 translocation and MnSOD upregulation. Since p53 is an transcription factor regulating MnSOD expression, and p53 phosphorylation is indicative of its functional activation [26–29], we proposed a possibility that p53 acted as a key factor. To confirm this, first we identified the p53 status by cDNA sequencing. The results showed that a wild-type p53 was expressed in the NB4 cells used in this study (data not shown). Then we extracted nuclear fractions of cells and detected the phosphorylation level of p53 (Ser15). Obviously, p53 phosphorylation was stimulated by selenite since 6 h and peaked at 9 h, while total

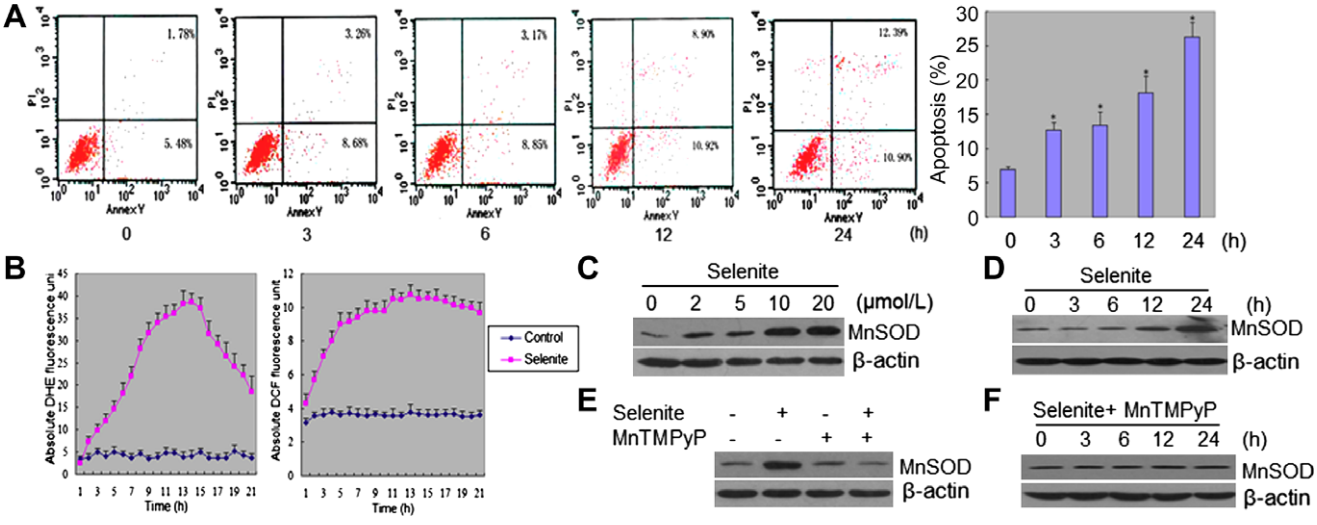

Fig. 1. MnSOD was upregulated through ROS in selenite-induced apoptosis. (A) Sodium selenite-induced apoptosis of NB4 cells. NB4 cells were treated with sodium selenite (20 μmol/l) for different time as indicated. Then apoptosis was analyzed by flow cytometry using Annexin V-FITC/PI staining. Data were presented as mean values with SD ($n = 3$), $^{*}P < 0.05$ compared with control group. (B) Selenite-induced ROS generation. NB4 cells were treated with sodium selenite (20 μmol/l). Intracellular superoxide or hydrogen peroxide was detected by DHE or DCF-based measurements respectively. Data were presented as mean values with SD ($n = 3$). (C) Selenite-induced MnSOD upregulation in a dose-dependent manner. Cells were treated with different doses of selenite as indicated for 24 h. Then MnSOD was detected by Western blot. (D) Selenite-induced MnSOD upregulation in a time-dependent manner. Cells were treated with selenite (20 μmol/l) for different time as indicated. Then MnSOD was detected by Western blot. (E) Effect of ROS scavenger on MnSOD upregulation at 24 h. Cells were pretreated with or without MnTMPyP (10 μmol/l) for 1h before selenite (20 μmol/l) exposure for 24 h. Then MnSOD was detected by Western blot. (E) Effect of ROS scavenger on MnSOD upregulation at different time points. Cells were pretreated with MnTMPyP (10 μmol/l) for 1 h before selenite (20 μmol/l) exposure for different time as indicated. Then MnSOD was detected by Western blot. The data were representative of at least three separate experiments.

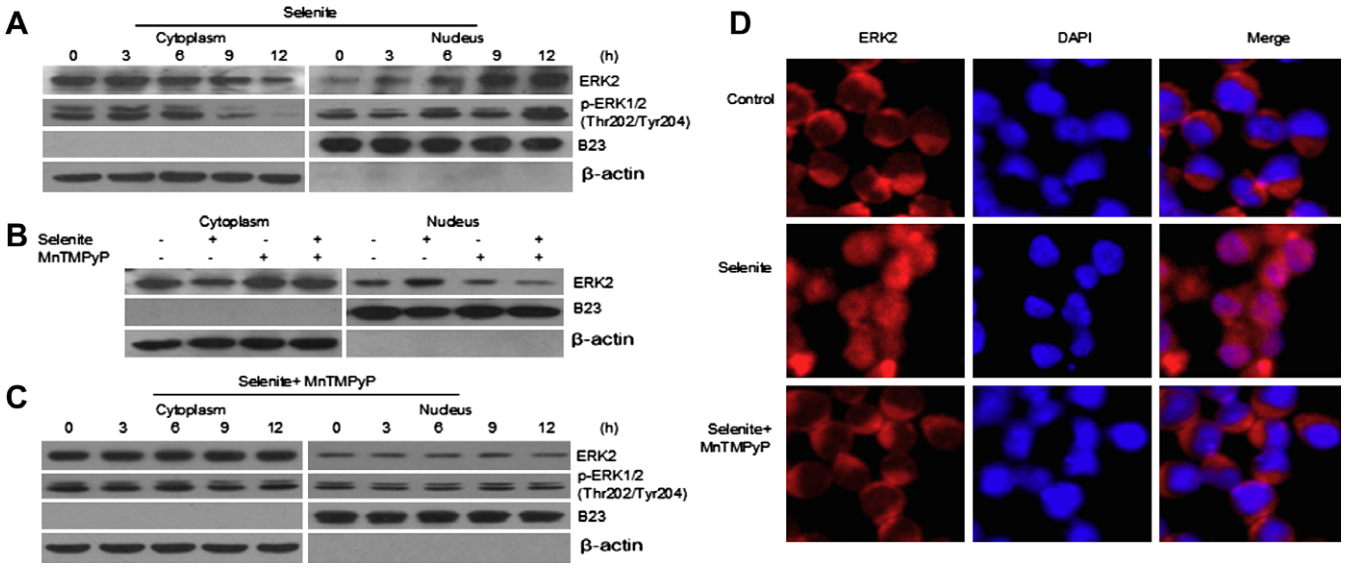

Fig. 2. Selenite-induced nuclear translocation of ERK2 through ROS. (A) Nuclear translocation of ERK2 induced by selenite. Cells were treated with selenite (20 μmol/l) for different time as indicated. Then cytoplasmic and nuclear fractions were extracted and ERK2 as well as p-ERK1/2 (Thr202/Tyr204) were detected by Western blot. β-actin and B23 were used as loading control of cytoplasmic and nuclear proteins respectively. (B) Effect of ROS scavenger on ERK2 translocation at 12 h. Cells were pretreated with or without MnTMPyP (10 μmol/l) for 1 h before selenite (20 μmol/l) exposure for 12 h. Then cytoplasmic and nuclear fractions were extracted and ERK2 was detected by Western blot. (C) Effect of ROS scavenger on ERK2 translocation at different time points. Cells were pretreated with or without MnTMPyP (10 μmol/l) for 1h before selenite (20 μmol/l) exposure for different time as indicated. Then cytoplasmic and nuclear fractions were extracted and ERK2 as well as p-ERK1/2 (Thr202/Tyr204) were detected by Western blot. (D) Nuclear translocation of ERK2 demonstrated by immunofluorescent staining. Cells were pretreated with or without MnTMPyP (10 μmol/l) for 1h before selenite (20 μmol/l) exposure for 12 h, then ERK2 was immunostained with its primary antibody and TRITC conjugated secondary antibody (red). The nucleus was labeled with DAPI (blue). The data were representative of at least three separate experiments.

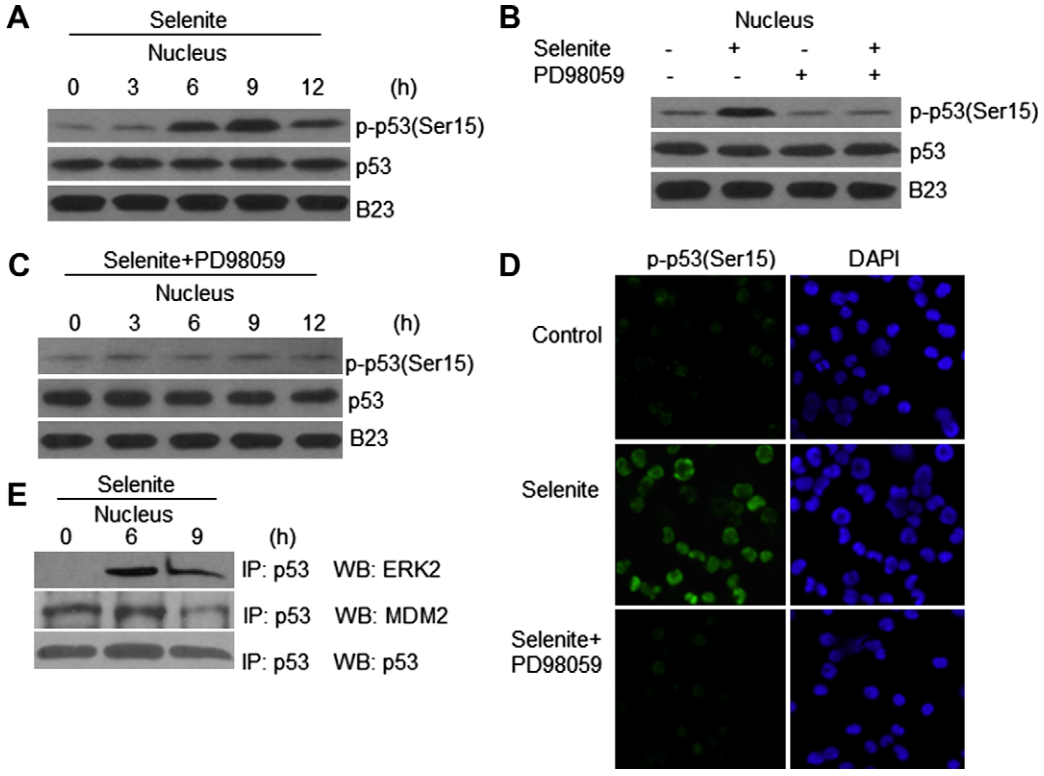

Fig. 3. ERK2 phosphorylated and activated nuclear p53 after its translocation. (A) Phosphorylation of nuclear p53 (Ser15) induced by selenite. Cells were treated with selenite (20 μmol/l) for different time as indicated before nuclear fractions were extracted. Then p-p53 (Ser15) and total p53 were detected by Western blot. B23 was used as loading control of nuclear proteins. (B) Effect of ERK inhibitor on nuclear p53 phosphorylation at 9 h. Cells were pretreated with or without PD98059 (20 μmol/l) for 1.5 h before selenite (20 μmol/l) exposure for 9 h. Then nuclear fractions were extracted. p-p53 (Ser15) and total p53 were detected by Western blot. (C) Effect of ERK inhibitor on nuclear p53 phosphorylation at different time points. Cells were pretreated with or without PD98059 (20 μmol/l) for 1.5 h before selenite (20 μmol/l) exposure for different time as indicated. Then nuclear fractions were extracted. p-p53 (Ser15) and total p53 were detected by Western blot. (D) Phosphorylation of p53 demonstrated by immunofluorescent staining. Cells were pretreated with or without PD98059 (20 μmol/l) for 1.5 h before selenite (20 μmol/l) exposure for 9 h, then p-p53 (Ser15) was immunostained with its primary antibody and FITC conjugated secondary antibody (green). The nucleus was labeled with DAPI (blue). (E) Interactions of p53 with ERK2 and MDM2 in the nucleus. Cells were treated with selenite (20 μmol/l) for different time as indicated. Then nuclear fractions were extracted and immunoprecipitated with p53 antibody, after which p53, ERK2 and MDM2 in the immunoprecipitated products were detected by Western blot. IP: immunoprecipitation, WB: Western blot. The data were representative of at least three separate experiments.

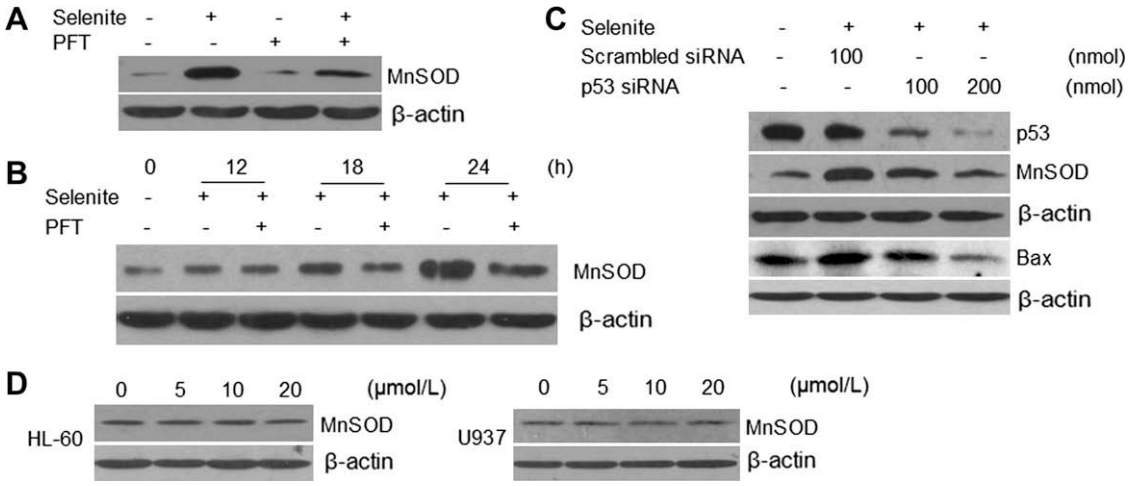

Fig. 4. Active p53 mediated upregulation of MnSOD. (A) Effect of p53 inhibitor on MnSOD upregulation at 24 h. Cells were pretreated with or without Pifithrin-α (PFT, 100 μmol/l) for 1.5 h before selenite (20 μmol/l) exposure for 24 h. Then MnSOD was detected by Western blot. (B) Effect of p53 inhibitor on MnSOD upregulation at different time points. Cells were pretreated with or without Pifithrin-α (100 μmol/l) for 1.5 h before selenite (20 μmol/l) exposure for different time as indicated. Then MnSOD was detected by Western blot. (C) Effect of p53 RNA interference on MnSOD and Bax expression. Cells were transfected twice with different doses of p53 siRNA or non-silencing scrambled siRNA respectively, followed by selenite (20 μmol/l) exposure for 24 h. Then MnSOD and Bax were detected by Western blot. (D) Effect of selenite on MnSOD expression in HL-60 and U937 cells. HL-60 or U937 Cells were treated with different doses of selenite as indicated for 24 h. Then MnSOD was detected by Western blot. The data were representative of at least three separate experiments.

nuclear p53 remained constant (Fig. 3A). This phosphorylation was thoroughly abolished by ERK inhibitor PD98059 (Fig. 3B and C), indicating ERK was responsible for this regulation. The participation of ERK in p53 phosphorylation was also demonstrated by immunofluorescent staining (Fig. 3D). Subsequently we performed immunoprecipitation of nuclear fractions with p53 antibody and detected p53 interactions with relative proteins. The results made clear an increased interaction between p53 and ERK2 as well as a contrary trend between p53 and MDM2 in the nucleus after selenite exposure (Fig. 3E), reflecting dissociation of p53 from MDM2 following association of p53 with ERK2.

3.4. Active p53 mediated upregulation of MnSOD

Then we explored whether the active p53 was involved in selenite-induced MnSOD upregulation. Pifithrin-α, a selective inhibitor for p53 was used to pretreat the cells before selenite exposure, and MnSOD upregulation was notably attenuated by this treatment (Fig. 4A and B). Likewise, p53 expression was inhibited by RNA interference, after which selenite-induced expression of MnSOD was weakened as well (Fig. 4C). In addition, bax, one of the p53-targeted genes, was also upregulated by selenite, which was blocked by p53 interference too (Fig. 4C), suggesting p53 exerted its transcriptional activity. Moreover, two other leukemia cell lines with different status of p53 were applied in this study. The HL-60 cell line has been definitely confirmed to lack p53 due to a major gene deletion [30–32], while the U937 cell line carries a mutant, inactive p53 resulted from deletion of 46 bases in p53 gene [33,34]. When treated with various doses of selenite, HL-60 and U937 cells showed no elevation of MnSOD (Fig. 4D), demonstrating that functional p53 is indispensable for selenite-induced MnSOD augment.

4. Discussion

It is shown by growing evidence that tumor cells and normal cells have different sensitivities to selenite treatment [35,36]. Our previous research has revealed apoptosis induced by selenite in leukemia-derived NB4 cells and colorectal cancer-derived SW480 cells. Moreover, our in vivo experiments indicated selenite inhibited colorectal tumor growth in mice without obvious adverse effects on body weights and activities [37], which is an encouraging finding suggesting selenite may find its way in the treatment of human tumors. Undoubtedly, before selenite can be safely applied to humans, some problems must be settled such as the appropriate dose and metabolic mechanisms in human body influencing its cellular effects.

Here in the present study, we found two intracellular ROS, superoxide and hydrogen peroxide were elevated immediately following selenite exposure. As a critical antioxidant enzyme removing superoxide free radicals, MnSOD remarkably increased during this process. MnSOD played a quite essential role in detoxification of the injurious ROS. Loss of MnSOD will result in serious events as aggravated endogenous oxidative stress or apoptosis [38,39], whereas its overexpression inhibits proline oxidase or radiation-induced apoptosis [40,41]. Therefore we postulated that upregulation of MnSOD presumably was a protective mechanism of NB4 cells under formidable threats of ROS. Previously we have already illuminated the vital role of ROS in selenite-induced apoptosis [4,6]. In this study, MnTMPyP totally reversed MnSOD upregulation, indicating ROS was also involved in the augment of MnSOD. Since MnTMPyP mainly targets superoxide radicals, we infer that superoxide, instead of hydrogen peroxide, is the most probable ROS responsible for selenite-induced apoptosis and MnSOD upregulation. Here as shown in Fig. 1B, the superoxide generation in NB4 cells was elevated immediately following selenite treatment, and peaked at approximately 12 h, after which it declined swiftly. Because MnSOD protein level started to increase since 12 h as shown in Fig. 1E, and its expression was reported to prohibit generation of superoxide radicals [42,43], it is reasonable to conclude that MnSOD upregulation, at least partially, participated in the decrease of superoxide level after 12 h. Therefore we hypothesize that a feedback relationship exists between MnSOD and ROS, especially the superoxide radicals. Selenite induced substantial superoxide generation in NB4 cells. As a result, superoxide caused upregulation of MnSOD, which removed the former in return.

As to the detailed mechanism how ROS mediated MnSOD upregulation, we found ERK played a significant role. ERK2 was translocated into the nucleus under the regulation of ROS,

therefore we infer ERK2 probably entered the nucleus to phosphorylate and activate one or more transcription factors targeting MnSOD gene. As a vital tumor suppressor, p53 exerted its antitumor effects mainly by transactivation of diverse target genes including Bax, Apaf-1 and caspase-6, or mitochondrial translocation to induce apoptosis independent of its transactivation ability [18,44,45]. As a target of p53, sod2 gene encoding MnSOD contains binding sites for p53 in the promoter, and its expression can be induced by p53 under certain stimuli such as doxorubicin treatment [19,20]. Although p53 is found mutated or depleted in various tumor cells, NB4 cells express a wild-type p53 confirmed by our cDNA sequencing analysis. Here we observed pronounced phosphorylation of nuclear p53 at Ser15 after selenite treatment, which was totally eliminated by ERK inhibitor. In addition, amount of total nuclear p53 was unaltered, thus ruling out nuclear translocation of p53 from the cytoplasm. Collectively, these results indicated that by virtue of nuclear translocation, ERK2 phosphorylated p53 in the nucleus. It has been validated p53 phosphorylation at Ser15 inhibits its interaction with the negative regulator MDM2, the product of an oncogene. Binding of MDM2 to p53 prohibits transactivation ability of p53 and targets p53 for proteasome-mediated degradation. Phosphorylation at Ser15 releases p53 from MDM2, promoting accumulation, DNA-binding property and functional activation of p53 [26–29]. Therefore, activation of nuclear p53 can be regarded as a significant consequence of ERK2 translocation. Moreover, immunoprecipitation of nuclear fractions revealed increased interaction between p53 and ERK2, as well as decreased interaction between p53 and MDM2 in response to selenite. We conclude from these results that without stimulus of selenite, nuclear p53 was associated with its inhibitory protein MDM2 and thus remained an inactive status. After selenite exposure, ERK2 entered the nucleus and phosphorylated p53 by direct contact, followed by the dissociation of p53 from MDM2, contributing to p53 activation.

To elucidate whether p53 was indeed involved in MnSOD upregulation, we used Pifithrin-α (PFT), a selective p53 inhibitor which blocks p53-dependent transactivation [46], as well as p53 siRNA interference. Both treatment attenuated selenite-induced MnSOD upregulation, indicating the role of p53 to facilitate MnSOD expression. We also noticed that in the leukemia cell lines with null or mutant p53 such as HL-60 and U937, selenite could not induce MnSOD elevation as in NB4 cells, substantiating the key role of functional p53 in selenite-induced MnSOD upregulation. In summary, p53 activation can be considered as the link connecting ERK2 translocation and MnSOD upregulation. Triggered by ROS, ERK2 was translocated from the cytoplasm into the nucleus, where it directly interacted with and phosphorylated p53 at Ser15. As a result, p53 dissociated from MDM2 and was activated to induce MnSOD upregulation, representing a possible protective mechanism of NB4 cells to counteract oxidative stress (Supplementary Fig. 2).

Acknowledgments

This work was supported by the grants from National Natural Science Foundation of China (No. 30770491 and No. 30970655), Natural Science Foundation of Beijing (No. 5082015 and No. 7032034), State Key Laboratory Special Fund (No. 2060204) and Ministry of Education, China for Doctor-training Unite (No. 20091106110025).

Appendix A. Supplementary data

Supplementary data associated with this article can be found, in the online version, at doi:10.1016/j.febslet.2010.03.040.

References

[1] Sanmartín, C., Plano, D. and Palop, J.A. (2008) Selenium compounds and apoptotic modulation: a new perspective in cancer therapy. Mini Rev. Med. Chem. 8, 1020–1031.
[2] Sinha, R. and El-Bayoumy, K. (2004) Apoptosis is a critical cellular event in cancer chemoprevention and chemotherapy by selenium compounds. Curr. Cancer Drug Targets 4, 13–28.
[3] Asfour, I.A., El Shazly, S., Fayek, M.H., Hegab, H.M., Raouf, S. and Moussa, M.A. (2006) Effect of high-dose sodium selenite therapy on polymorphonuclear leukocyte apoptosis in non-Hodgkin's lymphoma patients. Biol. Trace Elem. Res. 110, 19–32.
[4] Guan, L., Han, B., Li, Z., Hua, F., Huang, F., Wei, W., Yang, Y. and Xu, C. (2009) Sodium selenite induces apoptosis by ROS-mediated endoplasmic reticulum stress and mitochondrial dysfunction in human acute promyelocytic leukemia NB4 cells. Apoptosis 14, 218–225.
[5] Dong, H., Ying, T., Li, T., Cao, T., Wang, J., Yuan, J., Feng, E., Han, B., Hua, F., Yang, Y., Yuan, J., Wang, H. and Xu, C. (2006) Comparative proteomic analysis of apoptosis induced by sodium selenite in human acute promyelocytic leukemia NB4 cells. J. Cell. Biochem. 98, 1495–1506.
[6] Guan, L., Han, B., Li, J., Li, Z., Huang, F., Yang, Y. and Xu, C. (2009) Exposure of human leukemia NB4 cells to increasing concentrations of selenite switches the signaling from pro-survival to pro-apoptos. Ann. Hematol. 88, 733–742.
[7] Han, B., Wei, W., Hua, F., Cao, T., Dong, H., Yang, T., Yang, Y., Pan, H. and Xu, C. (2007) Requirement for ERK activity in sodium selenite-induced apoptosis of acute promyelocytic leukemia-derived NB4 cells. J. Biochem. Mol. Biol. 40, 196–204.
[8] Cao, T., Hua, F., Xu, C., Han, B., Dong, H., Zuo, L., Wang, X., Yang, Y., Pan, H. and Zhang, Z. (2006) Distinct effects of different concentrations of sodium selenite on apoptosis, cell cycle, and gene expression profile in acute promyeloytic leukemia-derived NB4 cells. Ann. Hematol. 85, 434–442.
[9] Zuo, L., Li, J., Yang, Y., Wang, X., Shen, T., Xu, C. and Zhang, Z. (2004) Sodium selenite induces apoptosis in acute promyelocytic leukemia-derived NB4 cells by a caspase-3-dependent mechanism and a redox pathway different from that of arsenic trioxide. Ann. Hematol. 83, 751–758.
[10] Culotta, V.C., Yang, M. and O'Halloran, T.V. (2006) Activation of superoxide dismutases: putting the metal to the pedal. Biochim. Biophys. 763, 747–758.
[11] Giovambattista, P., Renata, C., Barbara, B., Salvatore, F., Daniela, F., Silvia, B. and Tommaso, G. (2004) Mitochondrial superoxide dismutase: a promising target for new anticancer therapies. Curr. Med. Chem. 11, 1299–1308.
[12] Ramos, J.W. (2008) The regulation of extracellular signal-regulated kinase (ERK) in mammalian cells. Int. J. Biochem. Cell Biol. 283, 9248–9256.
[13] Baccarini, M. (2005) Second nature: biological functions of the Raf-1 ''kinase''. FEBS Lett. 579, 3271–3277.
[14] Ma, C., Bower, K.A., Chen, G., Shi, X., Ke, Z.J. and Luo, J. (2008) Interaction between ERK and GSK3beta mediates basic fibroblast growth factor-induced apoptosis in SK-N-MC neuroblastoma cells. J. Biol. Chem. 283, 9248–9256.
[15] Brunet, A., Roux, D., Lenormand, P., Dowd, S., Keyse, S. and Pouysségur, J. (1999) Nuclear translocation of p42/p44 mitogen-activated protein kinase is required for growth factor-induced gene expression and cell cycle entry. EMBO J. 18, 664–674.
[16] Ranganathan, A., Yazicioglu, M.N. and Cobb, M.H. (2006) The nuclear localization of ERK2 occurs by mechanisms both independent of and dependent on energy. J. Biol. Chem. 281, 15645–15652.
[17] Yazicioglu, M.N., Goad, D.L., Ranganathan, A., Whitehurst, A.W., Goldsmith, E.J. and Cobb, M.H. (2007) Mutations in ERK2 binding sites affect nuclear entry. J. Biol. Chem. 282, 28759–28767.
[18] Fridman, J.S. and Lowe, S.W. (2003) Control of apoptosis by p53. Oncogene 22, 9030–9040.
[19] O'Connor, J.C., Wallace, D.M., O'Brien, C.J. and Cotter, T.G. (2008) A novel antioxidant function for the tumor-suppressor gene p53 in the retinal ganglion cell. Invest. Ophthalmol. Vis. Sci. 49, 4237–4244.
[20] Hussain, S.P., Amstad, P., He, P., Robles, A., Lupold, S., Kaneko, I., Ichimiya, M., Sengupta, S., Mechanic, L., Okamura, S., Hofseth, L.J., Moake, M., Nagashima, M., Forrester, K.S. and Harris, C.C. (2004) P53-induced up-regulation of MnSOD and GPx but not catalase increases oxidative stress and apoptosis. Cancer Res. 64, 2350–2356.
[21] Pivoriūnas, A., Savickiene, J., Treigyte, G., Tunaitis, V., Navakauskiene, R. and Magnusson, K.E. (2007) PI 3-K signaling pathway suppresses PMA-induced expression of p21WAF1/Cip1 in human leukemia cells. Mol. Cell. Biochem. 302, 9–18.
[22] Ito, K., Nakazato, T., Yamato, K., Miyakawa, Y., Yamada, T., Hozumi, N., Segawa, K., Ikeda, Y. and Kizaki, M. (2004) Induction of apoptosis in leukemic cells by homovanillic acid derivative, capsaicin, through oxidative stress: implication of phosphorylation of p53 at Ser-15 residue by reactive oxygen species. Cancer Res. 64, 1071–1078.
[23] Ito, K., Nakazato, T., Miyakawa, Y., Yamato, K., Ikeda, Y. and Kizaki, M. (2003) Caffeine induces G2/M arrest and apoptosis via a novel p53-dependent pathway in NB4 promyelocytic leukemia cells. J. Cell. Physiol. 196, 276–283.
[24] Mata-Greenwood, E., Cuendet, M., Sher, D., Gustin, D., Stock, W. and Pezzuto, J.M. (2002) Brusatol-mediated induction of leukemic cell differentiation and G(1) arrest is associated with down-regulation of c-myc. Leukemia 16, 2275–2284.

[25] García-Cazarín, M.L., Smith, J.L., Clair, D.K. and Piascik, M.T. (2008) The alpha1D-adrenergic receptor induces vascular smooth muscle apoptosis via a p53-dependent mechanism. Mol. Pharmacol. 74, 1000–1007.
[26] Dias, S.S., Hogan, C., Ochocka, A.M. and Meek, D.W. (2009) Polo-like kinase-1 phosphorylates MDM2 at Ser260 and stimulates MDM2-mediated p53 turnover. FEBS Lett. 583 (22), 3543–3548.
[27] Tibbetts, R.S., Brumbaugh, K.M., Williams, J.M., Sarkaria, J.N., Cliby, W.A., Shieh, S.Y., Taya, Y., Prives, C. and Abraham, R.T. (1999) A role for ATR in the DNA damage-induced phosphorylation of p53. Genes Dev. 15, 152–157.
[28] Siliciano, J.D., Canman, C.E., Taya, Y., Sakaguchi, K., Appella, E. and Kastan, M.B. (1997) DNA damage induces phosphorylation of the amino terminus of p53. Genes Dev. 11, 3471–3481.
[29] Jaiswal, A.S. and Narayan, S. (2002) SN2 DNA-alkylating agent-induced phosphorylation of p53 and activation of p21 gene expression. Mutat. Res. 500, 17–30.
[30] Wolf, D. and Rotter, V. (1985) Major deletions in the gene encoding the p53 tumor antigen cause lack of p53 expression in HL-60 cells. Proc. Natl. Acad. Sci. USA 82, 790–794.
[31] Banerjee, D., Lenz, H.J., Schnieders, B., Manno, D.J., Ju, J.F., Spears, C.P., Hochhauser, D., Danenberg, K., Danenberg, P. and Bertino, J.R. (1995) Transfection of wild-type but not mutant p53 induces early monocytic differentiation in HL60 cells and increases their sensitivity to stress. Cell Growth Differ. 6, 1405–1413.
[32] Soddu, S., Blandino, G., Citro, G., Scardigli, R., Piaggio, G., Ferber, A., Calabretta, B. and Sacchi, A. (1994) Wild-type p53 gene expression induces granulocytic differentiation of HL-60 cells. Blood 83, 2230–2237.
[33] Sugimoto, K., Toyoshima, H., Sakai, R., Miyagawa, K., Hagiwara, K., Ishikawa, F., Takaku, F., Yazaki, Y. and Hirai, H. (1992) Frequent mutations in the p53 gene in human myeloid leukemia cell lines. Blood 79, 2378–2383.
[34] Kastan, M.B., Radin, A.I., Kuerbitz, S.J., Onyekwere, O., Wolkow, C.A., Civin, C.I., Stone, K.D., Woo, T., Ravindranath, Y. and Craig, R.W. (1991) Levels of p53 protein increase with maturation in human hematopoietic cells. Cancer Res. 51, 4279–4286.
[35] Husbeck, B., Nonn, L., Peehl, D.M. and Knox, S.J. (2006) Tumor-selective killing by selenite in patient-matched pairs of normal and malignant prostate cells. Prostate 66, 218–225.
[36] Nilsonne, G., Sun, X., Nystrom, C., Rundlof, A.K., Potamitou Fernandes, A., Bjornstedt, M. and Dobra, K. (2006) Selenite induces apoptosis in sarcomatoid malignant mesothelioma cells through oxidative stress. Free Radic. Biol. Med. 41, 874–885.
[37] Huang, F., Nie, C., Yang, Y., Yue, W., Ren, Y., Shang, Y., Wang, X., Jin, H., Xu, C. and Chen, Q. (2009) Selenite induces redox-dependent Bax activation and apoptosis in colorectal cancer cells. Free Radic. Biol. Med. 46, 1186–1196.
[38] Strassburger, M., Bloch, W., Sulyok, S., Schüller, J., Keist, A.F., Schmidt, A., Wenk, J., Peters, T., Wlaschek, M., Lenart, J., Krieg, T., Hafner, M., Kümin, A., Werner, S., Müller, W. and Scharffetter-Kochanek, K. (2005) Heterozygous deficiency of manganese superoxide dismutase results in severe lipid peroxidation and spontaneous apoptosis in murine myocardium in vivo. Free Radic. Biol. Med. 38, 1458–1470.
[39] Kirby, K., Hu, J., Hilliker, A.J. and Phillips, J.P. (2002) RNA interference-mediated silencing of Sod2 in Drosophila leads to early adult-onset mortality and elevated endogenous oxidative stress. Proc. Natl. Acad. Sci. USA 99, 16162–16167.
[40] Epperly, M.W., Sikora, C.A., DeFilippi, S.J., Gretton, J.A., Zhan, Q. and Kufe, D.W. (2002) Manganese superoxide dismutase (SOD2) inhibits radiation-induced apoptosis by stabilization of the mitochondrial membrane. Radiat. Res. 157, 568–577.
[41] Liu, Y., Borchert, G.L., Donald, S.P., Surazynski, A., Hu, C.A., Weydert, J., Oberley, L.W. and Phang, J.M. (2005) MnSOD inhibits proline oxidase-induced apoptosis in colorectal cancer cells. Carcinogenesis 28, 1335–1342.
[42] Fisher, C.J. and Goswami, P.C. (2008) Mitochondria-targeted antioxidant enzyme activity regulates radioresistance in human pancreatic cancer cells. Cancer Biol. Ther. 7, 1271–1279.
[43] Kanwar, M., Chan, P.S., Kern, T.S. and Kowluru, R.A. (2007) Oxidative damage in the retinal mitochondria of diabetic mice. possible protection by superoxide dismutase. Invest. Ophthalmol. Vis. Sci. 48, 3805–3811.
[44] Mihara, M., Erster, S., Zaika, A., Petrenko, O., Chittenden, T., Pancoska, P. and Moll, U.M. (2003) P53 has a direct apoptogenic role at the mitochondria. Mol. Cell 11, 577–590.
[45] Endo, H., Kamada, H., Nito, C., Nishi, T. and Chan, P.H. (2006) Mitochondrial translocation of p53 mediates release of cytochrome c and hippocampal CA1 neuronal death after transient global cerebral ischemia in rats. J. Neurosci. 26, 7974–7983.
[46] Komarov, R.G., Komarova, E.A., Kondratov, R.V., Christov-Tselkov, K., Coon, J.S., Chernov, M.V. and Gudkov, A.V. (1999) A chemical inhibitor of p53 that protects mice from the side effects of cancer therapy. Science 285, 1733–1737.